Electronic Supplementary Information

Mesoporous supraparticles with a tailored solid-liquid-gas interface for visual indication of H_2 gas and NH_3 vapours

*Andreas Zink,[†a] Jakob Reichstein,[†a] Nico Ruhland,[a] Nina Stockinger,[a] Boris S. Morozov,[b] Carlos Cuadrado Collados,[c] Matthias Thommes,[c] Evgeny A. Kataev,[b] Susanne Wintzheimer[ad] and Karl Mandel[*ad]*

[†] These authors contributed equally to this work.

[a] Department of Chemistry and Pharmacy, Inorganic Chemistry, Friedrich-Alexander-Universität Erlangen-Nürnberg (FAU), Egerlandstraße 1, D-91058 Erlangen, Germany; E-mail: karl.mandel@fau.de

[b] Department of Chemistry and Pharmacy, Organic Chemistry, Friedrich-Alexander-Universität Erlangen-Nürnberg (FAU), Nikolaus-Fiebiger-Str. 10, 91058 Erlangen, Germany

[c] Institute of Separation Science and Technology, Friedrich-Alexander-Universität Erlangen-Nürnberg (FAU), Egerlandstraße 3, D-91058 Erlangen, Germany.

[d] Fraunhofer-Institute for Silicate Research ISC, Neunerplatz 2, D-97082 Würzburg, Germany

Characterisation of supraparticle (SP) building blocks

Chromophore systems

Aiming at the identification of a suitable chromophore species for the targeted dual-gasochromic supraparticles (SPs) for H_2 and NH_3, a variety of commercially available redox indicator dyes was investigated (Fig. S1). The investigated dye species were resazurin (RES), methyl red (MR), methylene blue (MB), Reichardt's dye (RD), bromocresol green (BG), bromothymol blue (BTB), bromophenol blue (BPB), phenolphthalein (PPT), thymolphthalein (TPT) and tetrazolium red (TTZ).

The initial evaluation of their suitability for the targeted dual-gasochromic indicator functionality for H_2 and NH_3 vapour was performed in the liquid phase. Aqueous solutions (partially H_2O:EtOH mixtures) of the dye species were prepared, which revealed a roughly neutral pH. The influence of deprotonation and protonation on the colour of the chromophores was tested by adding an aqueous NH_3 solution (25%) and H_2SO_4 (96%) yielding roughly pH 10 and pH 2, respectively. The main findings can be summarized as follows:

MB and TTZ showed no significant change in their colour in the investigated pH range and are therefore not suitable for achieving the targeted functionality. All other dye solutions revealed the most pronounced colour change between an acidic environment (≈ pH 2) and a caustic environment (≈ pH 10) by NH_3-induced deprotonation of previously protonated to dye species. BG, BTB and BPB solutions showed a colour change from yellow (≈ pH 2) to blue (≈ pH 10). RD, PPT, TPT solutions switched from colourless (≈ pH 2) to a coloured state (≈ pH 10, RD and PPT: red, TPT: blue). RES and MR solutions revealed a colour change from red (≈ pH 2) to blue (≈ pH 10, RES) or yellow state (≈ pH 10, MR). Therefore, an acidic environment is most suitable for achieving a NH_3-induced colour change with high contrast.

Subsequently, the positively tested dye species, i.e., BG, BTB, BPB, RD, PPT, TPT, RES and MR were investigated regarding their ability to detect H_2 through a change in their colour. It was reported that dye solutions undergo a colour change upon H_2 dosing in the presence of catalytically active noble metal nanoparticles.[1] H_2 molecules adsorb and dissociate at their surface yielding active hydrogen. These H-species initiate a reduction of dye molecules. Therefore, the screening of the dyes for H_2-indication functionality was performed in an acidic dye solution and in the presence of small amounts of catalytically active Pt NPs (Fig. S2). H_2 gas (99,9%, Air Liquide) was introduced into the resulting dispersion via a cannula. Dispersions containing BG, BPB, RD, PPT and TPT did not show a H_2-induced colour change. Dispersions containing BPB and BTB showed a H_2-induced colour change that is however barely distinguishable from the NH_3-induced colour change. Therefore, BG, BPB, RD, PPT, TPT, BPB and BTB are not suitable for achieving the targeted functionality.

In contrast, the acidic RES dispersion showed initially an irreversible colour change from red to orange and blue and subsequently a reversible discolouration upon H_2 dosing (Fig. S1A1). This H_2-induced colour changes are attributed to the (ir)reversible reduction of protonated RES to protonated resorufin (RF) and hydroresorufin (hRF).[2] The red-colored acidic dispersion containing MR revealed a H_2-induced discolouration (Fig. S1B1), which is attributed to the irreversible reduction of MR.[1]

In sum, RES and MR were identified as most suitable indicator dyes for the targeted functionality. In an acidic dispersion containing Pt NPs, these dye species show distinguishable and pronounced colour changes upon H_2 dosing (UV-vis spectra and photographs, Fig. S1A1, B1) or the addition of NH_3 solution (UV-vis spectra and photographs, Fig. S1A2, B2), respectively.

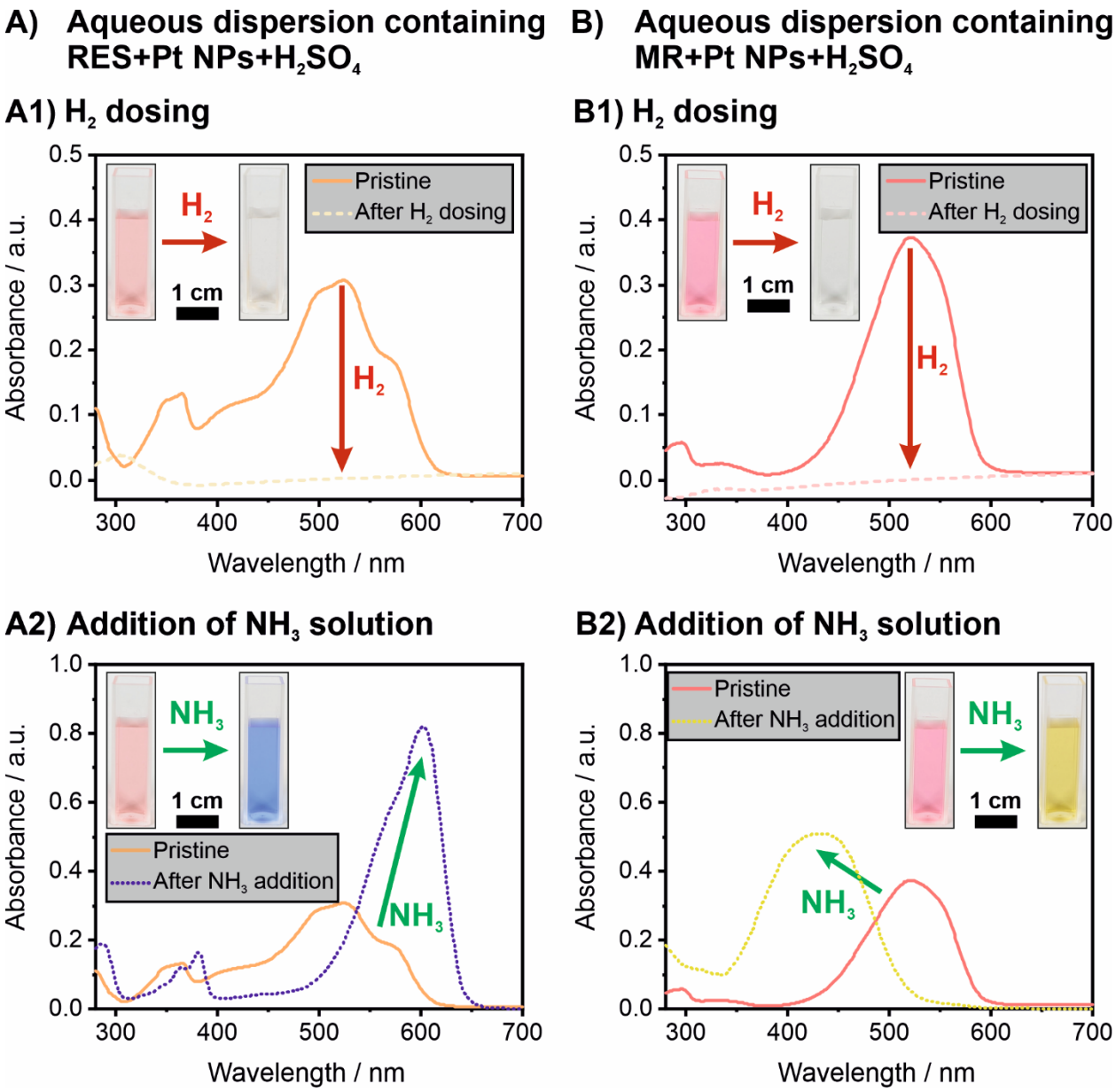

Fig. S1. (A-B) Comparison of UV-vis spectra of acidic aqueous dispersions (pH ≈2) containing Pt NPs, H_2SO_4, and the indicator dye RES (A) or MR (B) in their pristine state as well as after H_2 dosing (A1, B1) and the addition of an aqueous NH_3 solution (A2, B2). H_2- and NH_3-induced changes in the absorbance of the dispersions are indicated with coloured arrows and match the visual colour changes displayed in the photographs (insets).

Catalytically active Pt nanoparticles (NPs)

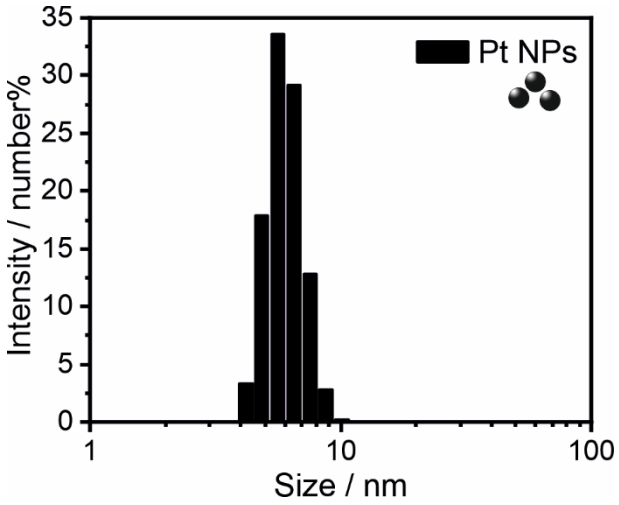

Fig. S2. Hydrodynamic particle diameter distribution of the Pt NPs used for the synthesis of the SPs obtained from dynamic light scattering measurements and displayed as number-weighted distribution. The distribution displays the average of three individual measurements.

Framework-building SiO_2 NPs

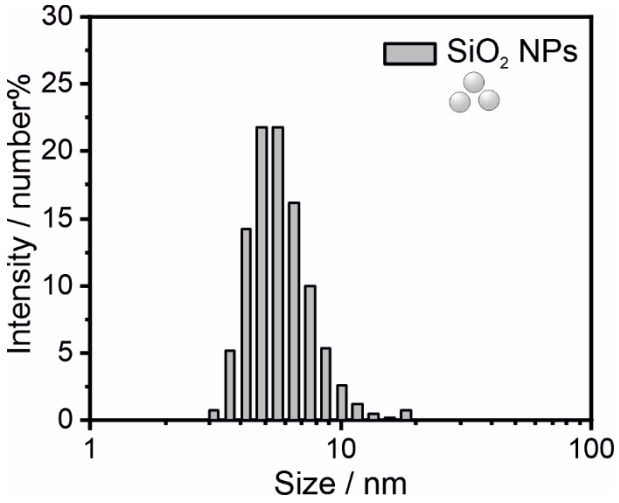

Fig. S3. Hydrodynamic particle diameter distribution of the SiO_2 NPs used for the synthesis of the SPs obtained from dynamic light scattering measurements and displayed as number-weighted distribution. The distribution displays the average of three individual measurements.

Structural and textural characterisation of supraparticles (SPs)

Two SP samples are investigated. Both are prepared from SiO_2 NPs (Fig S3), Pt NPs (Fig S2), and RES molecules, but without or with the addition of H_2SO_4. All components were mixed in one dispersion and subsequently spray-dried to a free-flowing powder consisting of SPs. The size distribution of the SPs was analysed via laser diffraction measurements (Fig. S4). The obtained size distributions are almost identical for both SP samples and range from approximately 2 to 8 µm. No significant effect of the addition of H_2SO_4 on the particle size distribution is observed.

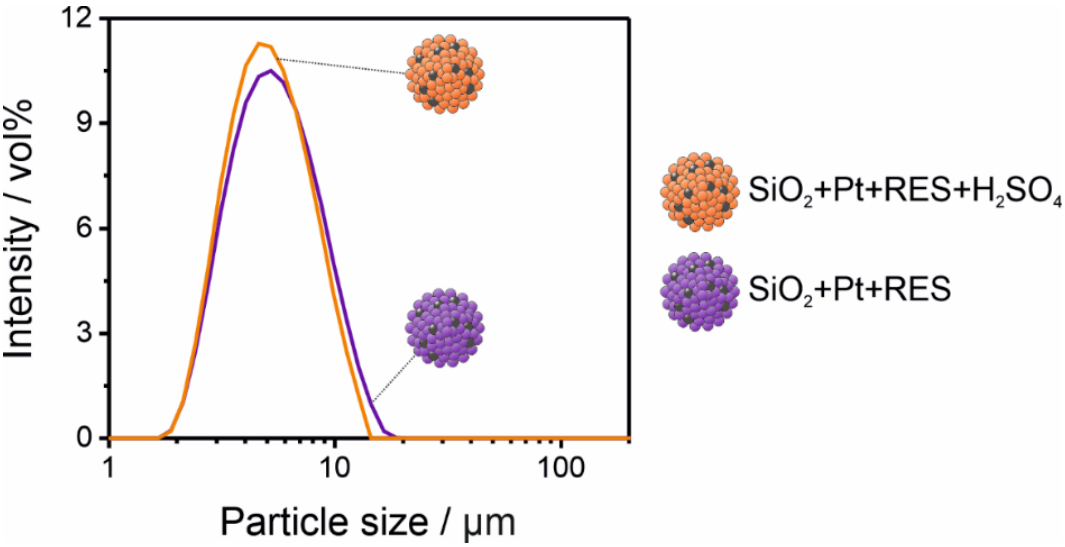

Fig. S4. Particle size distributions of the investigated SP samples consisting of SiO_2 NPs, Pt NPs, and RES molecules with and without the addition of H_2SO_4 obtained from laser diffraction measurements. Both types of SPs show an almost identical size distribution. The addition of H_2SO_4 to the mixed dispersion before spray-drying has no significant effect on the particle size distribution. The curves display the average of 5 individual measurements.

The textural properties of the SP samples were investigated via N_2 ad/desorption measurements at 77 K and evaluated regarding the influence of the addition of H_2SO_4 to the mixed dispersion prior to spray-drying. Both types of SPs exhibit an almost identically shaped type IV isotherm[3], which is characteristic for mesoporous materials and reveals pore condensation accompanied by hysteresis (Fig. S5A). In accordance with previous studies, these mesopores result from the interstitial space between the assembled NPs, i.e., mostly SiO_2 and few Pt NPs.[4,5] The saturation plateau of the isotherm extends in the relative pressure range($p \cdot p_0^{-1}$) from of 0.7 to 1 and indicates complete filling of the mesopores.

To investigated the pore size (Fig. S5B) and the pore volume distributions (Fig. S5C) of the SP samples, we applied the non-local density functional theory (NLDFT) method to the adsorption branch, by assuming cylindrical SiO_2 mesopores. The NLDFT pore size distribution of both samples is very similar and ranges from ≈ 2 to ≈ 8 nm. It is important to note that for SPs that were prepared in the presence of H_2SO_4 the formation of micropores (< 2 nm) is indicated, which however cannot be properly evaluated using N_2 ad-/desorption measurements. We assume that these micropores result from the pre-agglomeration of Pt and SiO_2 NPs due to colloidal destabilization induced by the addition of H_2SO_4 prior to the spray-

drying process.[6] This alteration in the NLDFT pore size distribution is also reflected in the NLDFT cumulative pore volume distribution of the SPs, which reveals a slight increase in total pore volume by adding H_2SO_4 before spray-drying.

The water adsorption capacity of the SPs was examined via water ad-/desorption analysis at standard temperature (298 K) and pressure (STP). Both SP samples show an almost identically shaped type IV isotherm with a hysteresis indicating pore condensation in the mesopores (Fig. S5D). The plateau region of both samples extends from a relative pressure of approximately 0.7 to 1. However, the presence of H_2SO_4 in the SPs increases the total water adsorption capacity and causes a small shift of the relative pressure range at which water condensation occurs to smaller values. We attribute these changes mainly to the hygroscopic nature of H_2SO_4[7] with an additional contribution from the observed formation of micropores in the SPs with H_2SO_4.

In sum, the addition of H_2SO_4 leads to the minor changes in the texture of the SPs and enhances their water adsorption capacity.

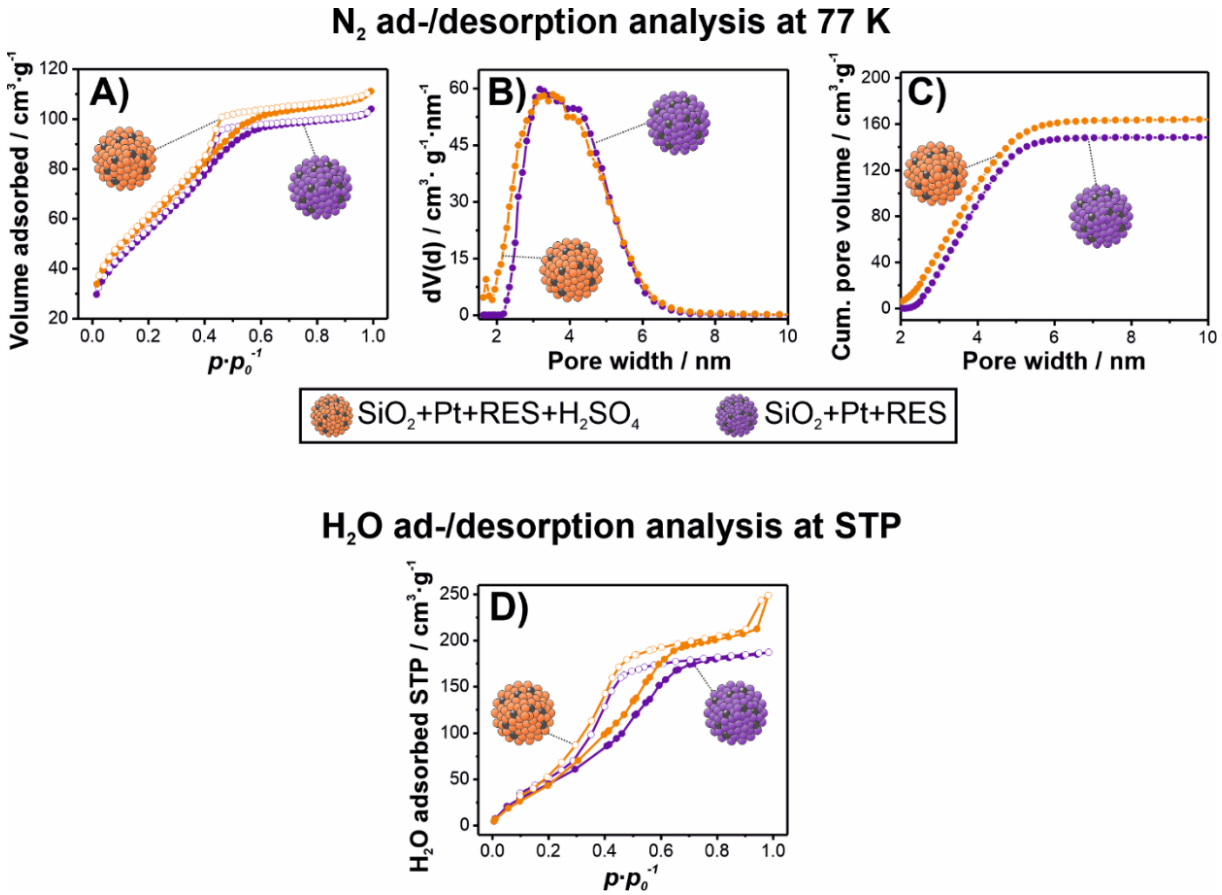

Fig. S5. Textural analysis of the investigated SP samples SiO_2 NPs, Pt NPs, and RES molecules with and without the addition of H_2SO_4: (A) N_2 ad-/desorption isotherms at 77 K. Full symbols indicate adsorption branch and empty symbols indicate desorption branch. (B) Nonlocal density functional theory (NLDFT) pore size distributions. (C) NLDFT cumulative pore volumes. (D) H_2O ad-/desorption isotherms at standard temperature (298 K) and pressure (STP). Full symbols indicate adsorption branch and empty symbols indicate desorption branch. The displayed H_2O isotherms display the 2nd ad-/desorption cycle.

Characterisation of the gasochromic functionality of the SPs

SP powder containing SiO_2 NPs, Pt NPs and RES molecules but no H_2SO_4 without *ex situ* H_2O dosing undergoes a rapid, eye-readable, two-step (ir)reversible colour change upon H_2 dosing (Fig. S6A1). However, no complete conversion to a colourless powder is observed and the powder remains partially pink. The H_2-induced colour change is associated to the irreversible reduction of deprotonated RES (purple) to deprotonated RF (pink), followed by a reversible reduction to hRF (colourless, Fig. S6A2).[1] In accordance with our previous studies,[4,5] the incomplete conversion from RF to hRF is attributed to the lower dye mobility compared to the SP powder after *ex situ* H_2O dosing (Fig. 2A1, main manuscript). Upon NH_3 vapour dosing, SPs without H_2SO_4 show no colour change (Fig. S6A3).

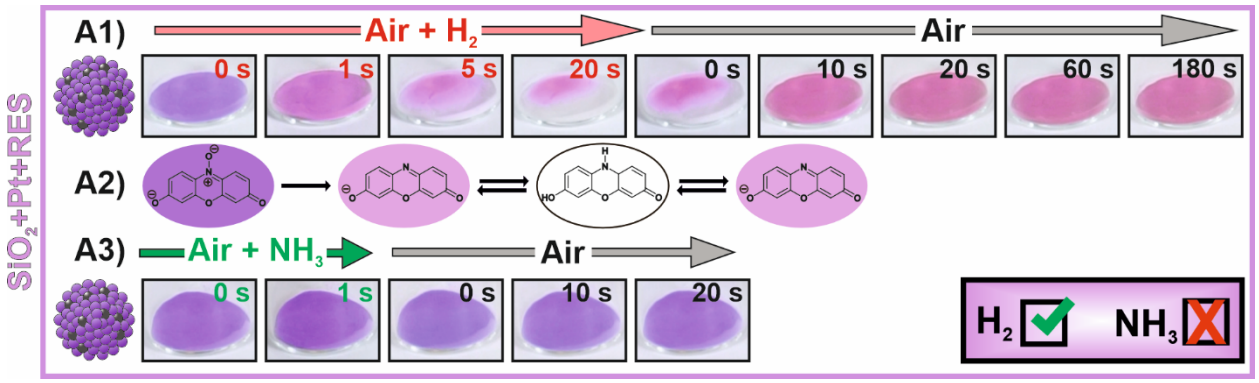

Fig. S6. (A1-3) Colour change reactions of the SPs containing SiO_2 NPs, Pt NPs and RES molecules without the addition of H_2SO_4 and without pretreatment (*ex situ* H_2O dosing): (A1) snapshots of the SP powder during H_2 dosing yielding an (ir)reversible two-step, eye-readable colour change. (A2) This colour change is caused by the irreversible H_2-induced conversion of RES to RF and the subsequent reversible conversion of RF to hRF, and vice versa. (A3) snapshots of the SP powder during NH_3 dosing yielding no visible colour change.

SP powder containing Pt NPs, SiO_2 NPs, RES and H_2SO_4 showed rapid, eye-readable, gas-specific colour change reactions upon exposure to H_2 or NH_3 vapours (Fig S7, ESI‡). First reaction with H_2 irreversibly reduced the orange RES-H^+ to the slightly brighter RF-H^+ (Fig. S7A1-A3). This is confirmed by distinct changes in their absorption and fluorescence spectra (Fig. S8, ESI‡). Further H_2 dosing led to blue powder due to the formation of a scarcely reported stable radical state of hRF (hRF·, Fig. S7A3)[2]. When the dye mobility was high enough, hRF· was further reduced by H_2 dosing to colourless hRF (Fig S7A2). After stopping H_2 dosing, the colourless SP powder (hRF) turned blue (hRF·), before reaching a final orange colour (RF-H^+). It is important to mention that the colouration of these SPs occurred at a much slower pace (up to 180 s) compared to their reduction (≈ 5-10 s) and the colouration of SPs without H_2SO_4 (≈ 5-10 s). We attribute this slow reversibility to the stability of the blue hRF· radical in air.

In contrast to H_2 dosing, NH_3 vapours induced a rapid, visual colour change of SPs containing H_2SO_4 from orange to purple (Fig. S7B1, B2) due to deprotonation of RES-H^+ to RES (Fig. S7B3). This reaction is caused by a pH increase of the liquid phase in the mesopores of the SPs that is likely induced by the adsorption and dissolution of gaseous NH_3 species.

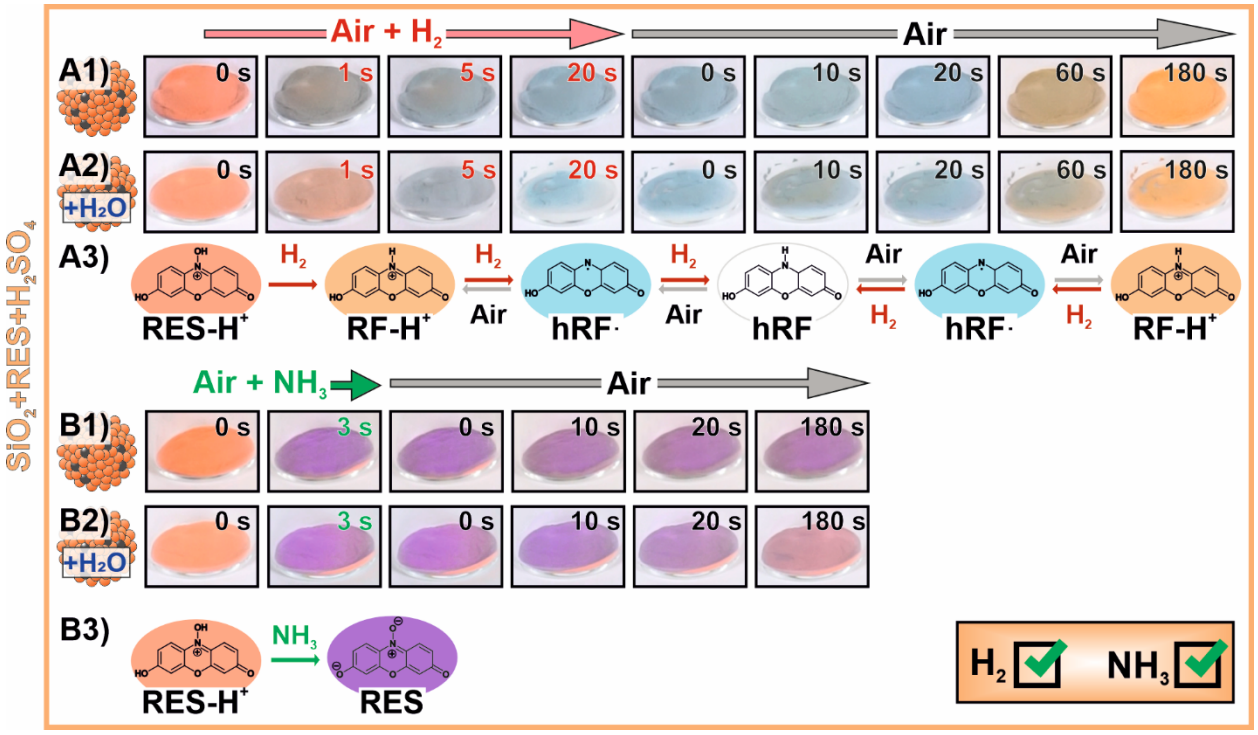

Fig. S7. A1-A2) Snapshots of SP powder containing SiO_2 NPs, Pt NPs and RES molecules and H_2SO_4 before (A1) and after *ex situ* H_2O dosing (A2) before, during and after H_2 dosing. A3) Reaction network for the observed H_2-induced colour change reaction. B1-B2) Snapshots of the same SPs before (B1) and after *ex situ* H_2O dosing (B2) before, during and after NH_3 dosing. B3) Reaction network for the observed NH_3-induced colour change reaction. These SPs demonstrate a proof-of-concept for dual-gasochromic SPs for of H_2 and NH_3.

Fluorescence spectroscopy analysis of SP powders

To support the proposed reaction mechanisms, the gasochromic indicator SPs are investigated via fluorescence spectroscopy in their pristine state as well as after an exposure to H_2 gas and NH_3 vapour, respectively (Fig. S8).

SPs prepared from SiO_2 NPs, Pt NPs and RES without the addition of H_2SO_4 did not show a colour change upon NH_3 dosing (Fig. 2C) due to the presence of deprotonated RES molecules in the pristine state of the SPs. Therefore, only SPs before (purple) and after H_2 dosing (pink) were investigated (Fig. S8 A). The fluorescence spectra were measured using an excitation wavelength of 365 nm. The absorption spectra were measured at the respective emission maximum of the two different SP powders. The emission spectrum of the basic sample shows a peak of the emission band around 644 nm (Fig. S8 A1), which is characteristic of RES and reveals a slight shift compared to RES solutions.[8–10] After H_2 dosing, a strong reduction of peak at 644 nm and the formation of a second emission band peaking around 585 nm is observed indicative of the formation of RF.[8–10] The co-existence of the two emissions demonstrates that the H_2 dosing did not achieve a complete conversion of all RES molecules to RF. The H_2-induced formation of RF is furthermore confirmed by the detected changes in the excitation spectra of the SPs (Fig. S8 A2). The spectrum of pristine SPs shows two characteristic absorption bands stemming from the ππ* transition of the phenoxazin-3-one at around 600 nm and to the weak nπ* transitions of the N-oxide at around 380 nm, respectively.[10] The altered excitation spectrum of SPs after H_2 dosing confirms the H_2-induced conversion of RES to RF most prominently by showing a strong reduction of the nπ* transition of the N-oxide at around 380 nm.

Next, SPs consisting of SiO_2 NPs, Pt NPs, RES and H_2SO_4 are investigated in their pristine state (orange) as well as after NH_3 and H_2 dosing, respectively (Fig. S8B). In their pristine state (orange), the SPs exhibit an emission maximum at around 612 nm (Fig. S8B1), which is significantly shifted (roughly 30 nm) compared to the SPs with deprotonated RES. After exposure to NH_3 vapour (purple), the emission peak (Fig. S8B1) and the absorption band of the nπ* transitions of the N-oxide at around 350 nm (Fig. S8B2) of the SPs undergo bathochromic shifts (red shifts) to roughly 644 nm and 380 nm, respectively. In accordance with the literature[10] and the previous investigation of SPs without H_2SO_4 (Fig. S8A), these shifts are attributed to the NH_3-induced deprotonation of protonated RES (RES-H^+) and thus confirm the presence of RES-H^+ in the pristine state of the SPs.

SPs after exposure to H_2 (light orange) show a hypsochromic shift (blue shift) of the emission maximum, the emergence of an additional shoulder emerges at around 562 nm (Fig. S8B1) as well as a significant reduction of the absorption band at around 350 nm (Fig. S8B2). All of these observations are indicative of the H_2-induced conversion of protonated RES (RES-H^+) to protonated RF (RF-H^+)[10] and thus support the proposed reaction mechanism.

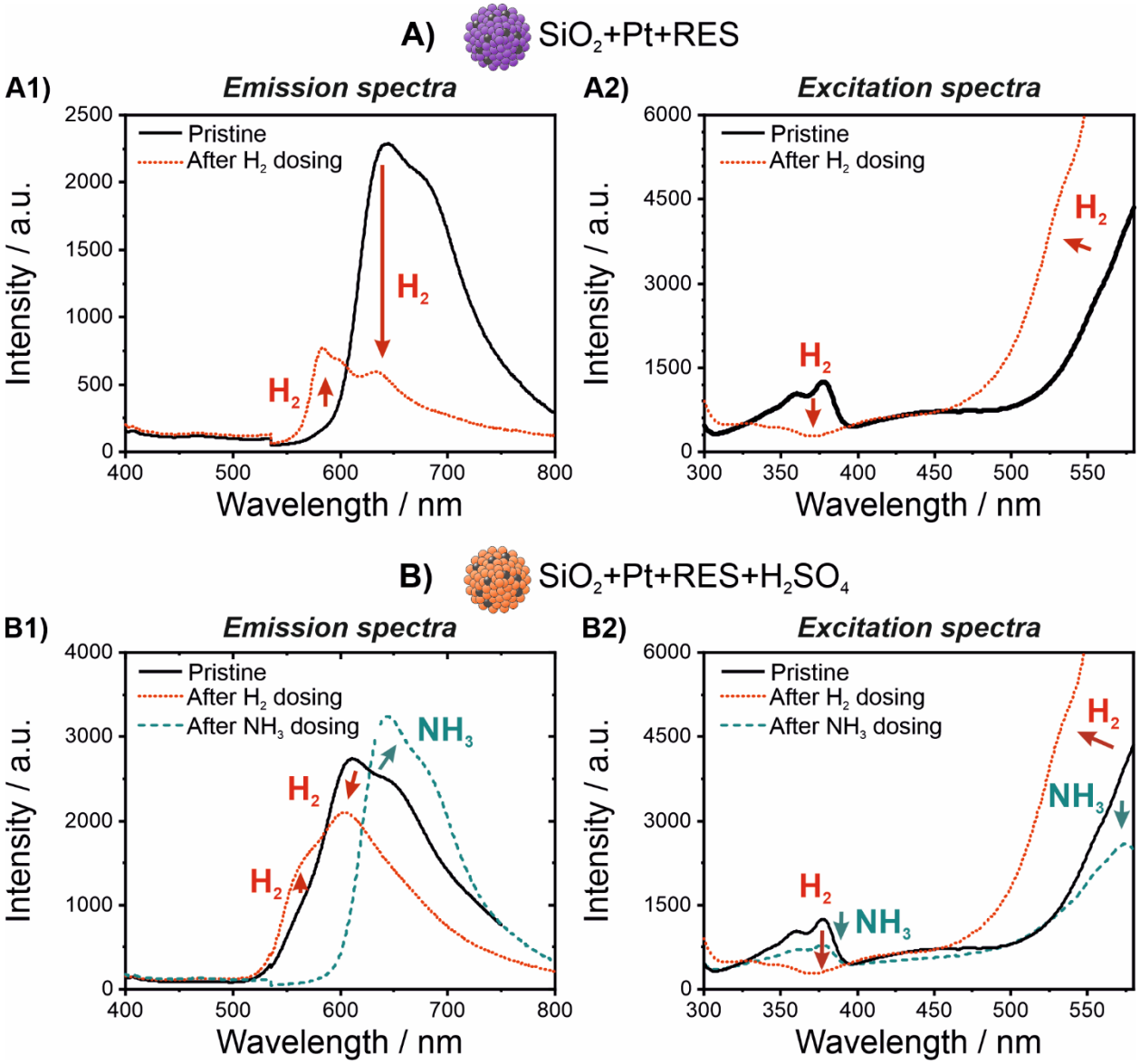

Fig. S8. (A-B) Fluorescence spectroscopy analysis of SPs containing SiO_2 NPs, Pt NPs and RES molecules without (A) and with the addition of H_2SO_4 (B): A1) fluorescence spectra (λ_{exc} = 365 nm) and A2) excitation spectra (monitoring the respective emission maximum) of pristine SPs and SPs after H_2 dosing. B1) fluorescence spectra (λ_{exc} = 365 nm) and B2) excitation spectra (monitoring the respective emission maximum) of pristine SPs as well as SPs after H_2 dosing or NH_3 dosing.

Mechanistic control experiment

As additional support for the proposed mechanisms, a control SP sample containing SiO_2 NPs, RES, H_2SO_4 but no Pt NPs was prepared and subjected to H_2 and NH_3 dosing, respectively. This sample showed no response upon H_2 dosing (Fig. S9A1) but an identical colour change from orange to purple upon NH_3 vapour dosing (Fig. S9A2) due to deprotonation of the incorporated RES-H^+ species (Fig. S9A3), which supports the proposed mechanisms of the NH_3 detection.

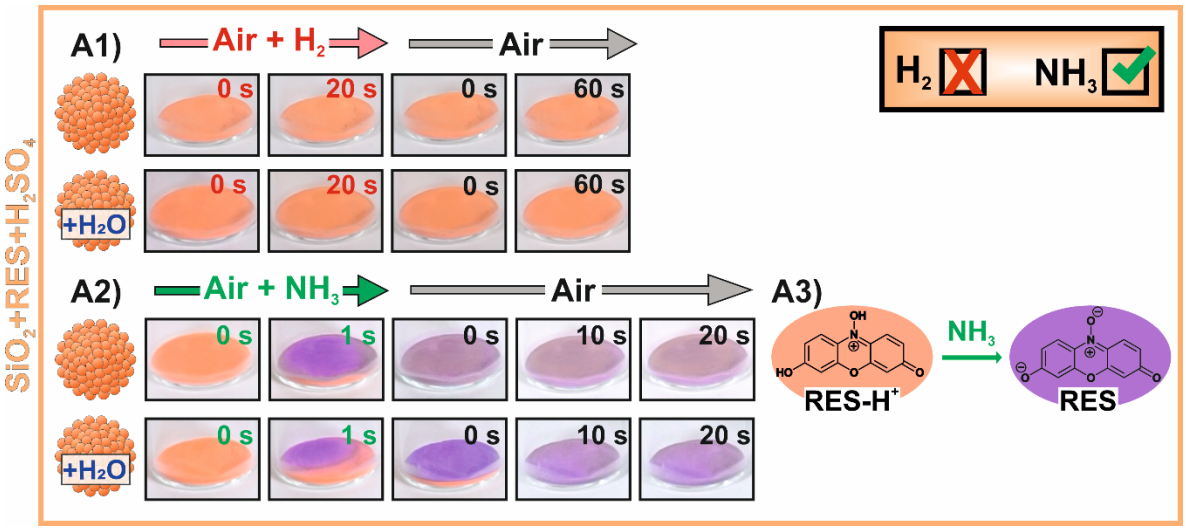

Fig. S9. (A1-3) Colour change reactions of the SPs containing SiO_2 NPs, RES molecules, H_2SO_4 but no Pt NPs without (top row) and after *ex situ* H_2O dosing (bottom row): (A1) snapshots of the SP powder during H_2 dosing yielding no visible colour change. (A2) snapshots of the SP powder during NH_3 dosing yielding an eye-readable and only partially reversible colour change from orange to purple. (A3) This colour change is caused by the alteration of pH within the liquid phase hosted in the mesopores of the SP due to the adsorption and dissolution of NH_3 vapour and the subsequent deprotonation of RES-H^+ species.

Investigation of the reversibility of the NH_3-induced colour change reaction of the SP powders

The NH_3-induced colour change of the SP powders is partially irreversible at ambient conditions, as the initially orange colour related to RES-H^+ was never fully recovered (Fig. 3B4, B5). However, when comparing the NH_3-induced colour change of the SP powder in its pristine state (Fig. 3B4) and after previous *ex situ* H_2O dosing *(Fig. 3B5)*, a slight difference in their degree of reversibility is detected. To investigate this difference in more detail, the two powders were subject to repeated NH_3/air dosing (Fig. S10), including three cycles of NH_3 dosing (3 s) and subsequent air dosing (2-3 min).

Comparing the reversibility of the colour change upon repeated NH_3/air dosing revealed a slightly higher degree of reversibility for SPs after *ex situ* H_2O dosing (Fig. S10b) compared to pristine SPs (Fig. S10a). The colour of pristine SP powder during and after NH_3 dosing can hardly be differentiated by the naked eye (Fig. S10a). In contrast, the SP powder after *ex situ* H_2O dosing recovers a brownish colour during air dosing, which is distinguishable from the purple colour during NH_3 dosing (Fig. S10b). This higher degree of reversibility is attributed to the enhanced amount of water in the SPs after *ex situ* H_2O dosing, which increases the amount of NH_3 required to alter the pH of the liquid phase in the mesopores in the same manner.

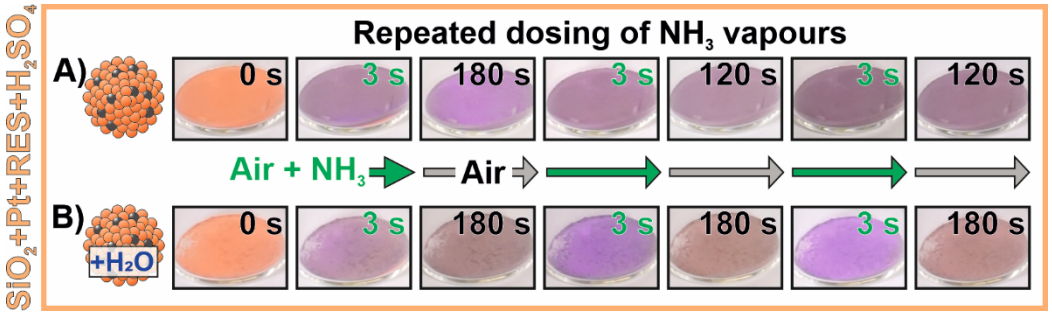

Fig. S10. (A-B) Snapshots of the colour change reactions of SPs containing SiO_2 NPs, Pt NPs, RES molecules and H_2SO_4 before (A) and after *ex situ* H_2O dosing (B) upon repeated NH_3 dosing (green arrows, green lettering) due to deprotonation of RES-H^+ (orange powder). The NH_3 dosing steps were interrupted by 2-3 min air dosing steps (grey arrows, black lettering). Both SP powders show a partially reversible colour change upon NH_3 dosing with subsequent exposure to air. The SP powder after *ex situ* H_2O dosing reveals a higher degree of reversibility. However, the original orange colour of the SP powders, related to the RES-H^+, was not recovered even after hours of air dosing. It is important to note that these experiments were performed on aged SP powders (3 months after their synthesis).

Investigation of the gasochromic functionality of the SPs upon simultaneous dosing of H_2 and NH_3

Besides testing separate H_2 and NH_3 dosing, the SPs containing Pt NPs, SiO_2 NPs, RES and H_2SO_4 were subjected to simultaneous exposure to both target species (Fig. S11A). When H_2 gas reacted with the SPs first, the irreversible reduction of RES-H^+ (orange) to RF-H^+ (bright orange) and the reversible reduction of RF-H^+ to hRF· (blue) were induced. However, as soon as NH_3 vapours were dosed, the reduction reaction stopped and impeded the formation of hRF due to poisoning of the incorporated Pt NPs by NH_3.[11] Therefore, instead of hRF (colourless), RF (pink) was formed by deprotonation of RF-H^+ upon simultaneous dosing of H_2 gas and NH_3 vapours. Subsequent, H_2 dosing did not change the colour of the SP powder due to the NH_3-poisoning that remained for several minutes at ambient conditions.
This reaction mechanism was confirmed by consecutive dosing of H_2 gas and NH_3 vapours, which also results in a pink powder related to the formation of RF (Fig. S11B). The NH_3-poisoning of the incorporated Pt NPs was confirmed by consecutive dosing of NH_3 vapours and H_2 gas, which yields a purple powder related to the formation of RES (Fig. S11C).

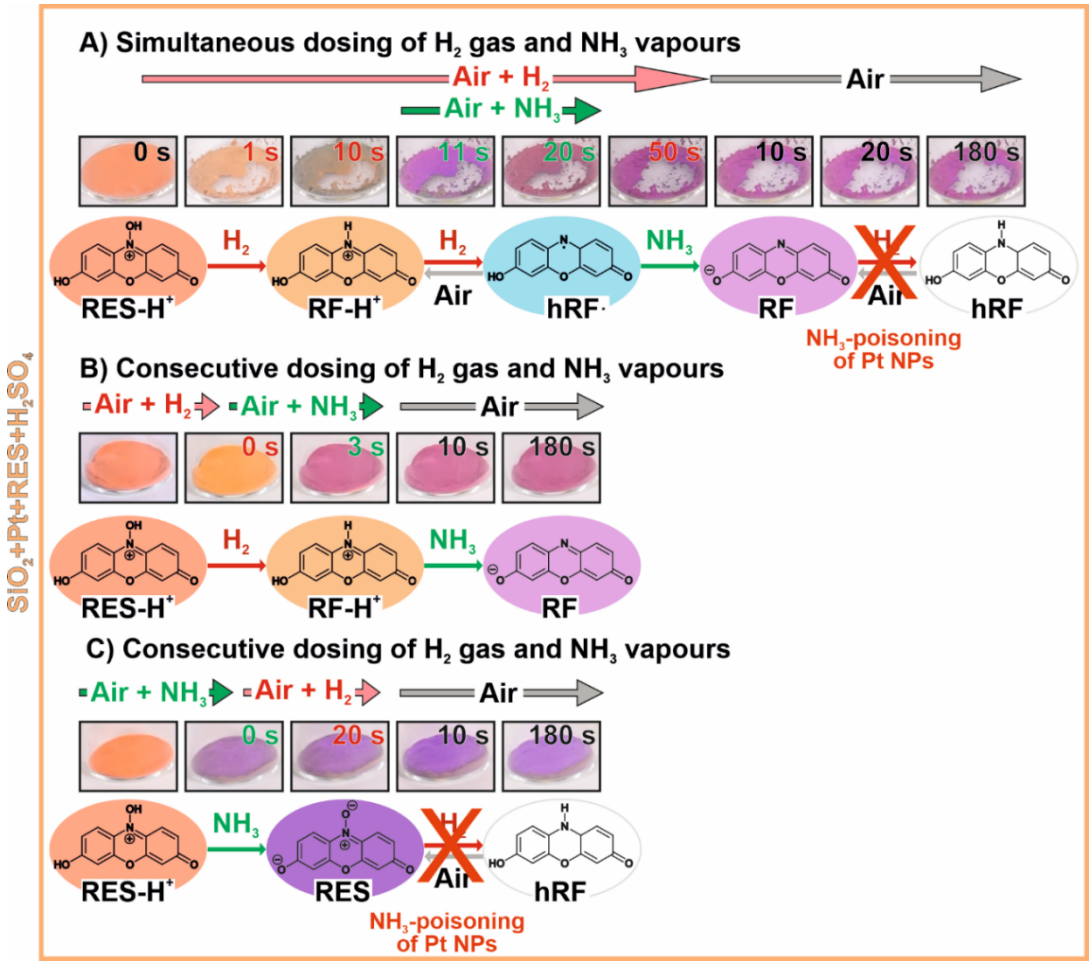

Fig. S11. A-C) Snapshots of the colour change reactions of SPs containing SiO_2 NPs, Pt NPs, RES molecules and H_2SO_4 upon simultaneous dosing of H_2 gas and NH_3 vapours (A), consecutive dosing of H_2 gas and NH_3 vapours (B), and consecutive dosing NH_3 vapours and H_2 gas, respectively. It is important to note that the simultaneous gas dosing experiment (A) was performed on aged SP powders (3 months after their synthesis).

Functional characterisation of supraparticles equipped with MR

The adjustability of the conceptualised SPs by exploiting their modular synthesis was exemplarily studied by exchanging the employed chromophore. Therefore, SPs containing SiO_2 NPs, Pt NPs, H_2SO_4 and MR were synthesized via spray-drying, yielding a red powder, indicative of protonated MR (MR-H^+). Their gasochromic functionality was probed analogously to the SPs containing RES (Fig. 2, main manuscript).
The pristine SP powder revealed no colour change in the presence of H_2 (Fig. S12A1, top row). In contrast, SP powder after *ex situ* water dosing revealed the expected H_2-induced irreversible discolouration (Fig. S12A1, bottom row), which was also observed in aqueous MR solutions (Fig. S1a). We attribute the absence of a colour change for pristine SPs to the limited of MR molecules when the pores are not sufficiently filled with water. The observed discolouration of the SPs results from the H_2-induced irreversible reduction of MR-H^+ to colourless N,N-dimethyl-*p*-phenylenediamine (DMPD) and anthranilic acid (Fig. S12A2).[1,12] In the presence of NH_3 vapours, the red SP powder turned irreversibly yellow within seconds independent of the pretreatment (Fig. S12A3). This colour change matches the observations from aqueous MR solution studies (Fig. S1b) and is attributed to the deprotonation of MR-H^+ to MR (Fig. S12A4).

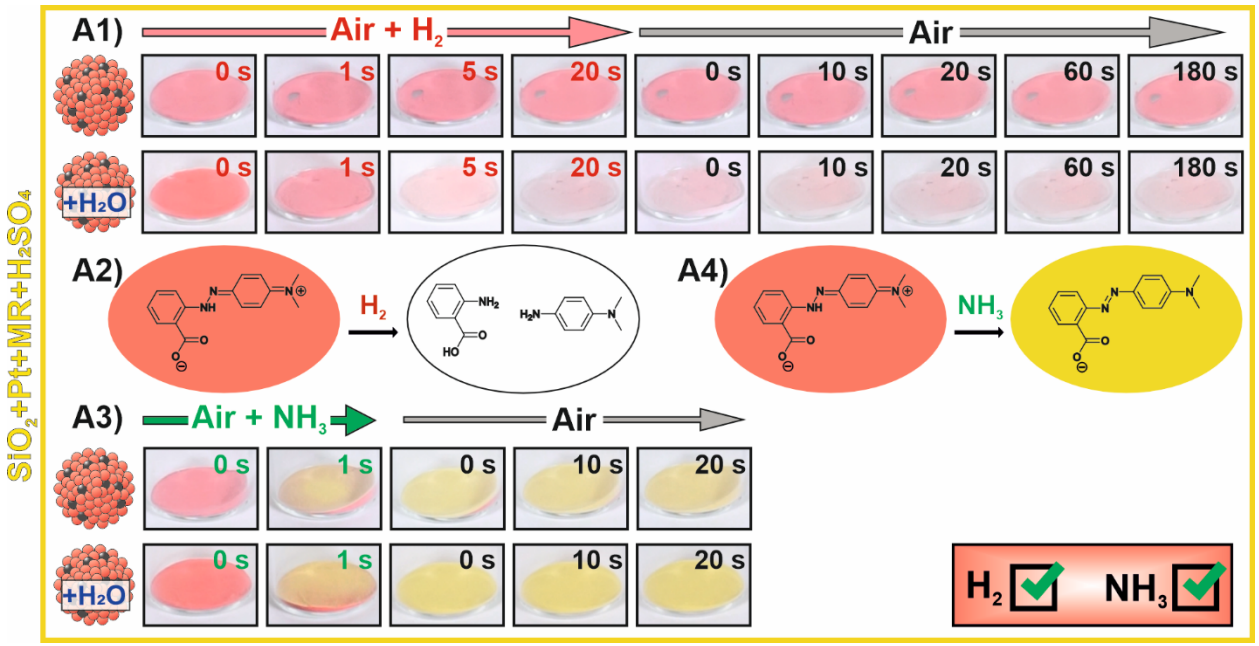

Fig. S12. (A1-A3) Colour change reactions of SPs containing SiO_2 NPs, Pt NPs, H_2SO_4 and MR: (A1, A3) snapshots of the SP powder without (top row) and with additional *ex situ* H_2O (bottom row) during H_2 dosing (A1) and NH_3 dosing (A3), respectively. (A2, A4) suggested reaction networks for the observed colour change reactions.

In situ UV-vis reflectance spectroscopy on SP powders exposed to varying gas atmospheres

A preliminary quantitative assessment of the dual-gasochromic indicator SPs based on RES and MR was performed via *in situ* UV-vis reflectance spectroscopy measurements. In the spectrometer, the SP powders were exposed to varying gas atmospheres (for 5 min each) while their absorption was permanently monitored in the wavelength range 800-350 nm using a reflectance measurement setup.

The spectrum of pristine SPs with RES-H^+ (orange) shows two characteristic absorption bands stemming from the ππ* transition of the phenoxazin-3-one at around 500 nm and the weak nπ* transitions of the N-oxide at around 350 nm, respectively (Fig. S13A).[10] Upon gas dosing with 2 vol% H_2 in N_2, both absorption bands vanished due to the reduction of RES-H^+ to colourless hRF. The ππ* transition of the phenoxazin-3-one at around 500 nm formed again after stopping the H_2 dosing. The absorption band at around 350 nm was irreversibly eliminated, which is indicative of the H_2-induced irreversible conversion of RES-H^+ to RF-H^+ (light orange). Upon subsequent gas dosing with roughly 620 ppm NH_3 in N_2, the absorption band at 500 nm showed a significant peak shift to roughly 550 nm accompanied by peak broadening. This is attributed to the NH_3-induced deprotonation of RF-H^+ (light orange) to RF (pink). Subsequent air dosing did not affect the final pink colour of the SPs.

The spectrum of pristine SPs with MR-H^+ (red) showed a strong absorption band peaking around 500 nm (Fig. S13B). Upon dosing with roughly 620 ppm NH_3 in N_2, the absorption band at 500 nm showed a slight reduction while the absorption in the wavelength range from 350 to 450 nm increases. In accordance with the study on aqueous MR solutions (Fig. S1b), this change in the absorption characteristics of the SPs is attributed to the NH_3-induced deprotonation of MR-H^+ to MR. These absorption characteristics remained unchanged upon subsequent air dosing. The following H_2 dosing with 2 vol% H_2 in N_2 eliminates the absorption bands almost completely due to the irreversible reduction of MR to DMPD and anthranilic acid (compare Fig. S12A1).[1,12]

In sum, the preliminary quantitative *in situ* UV-vis measurements demonstrated that dual-gasochromic SPs based on RES and MR undergo pronounced colour change reactions when they are exposed to ≈ 2 vol.% H_2 in N_2 (i.e., below the lower flammability limit of 4 vol.%[13]) or ≈ 620 ppm NH_3 in N_2 (i.e., below the limit where coughing, laryngospasm, and edema of the glottic region start[14]).

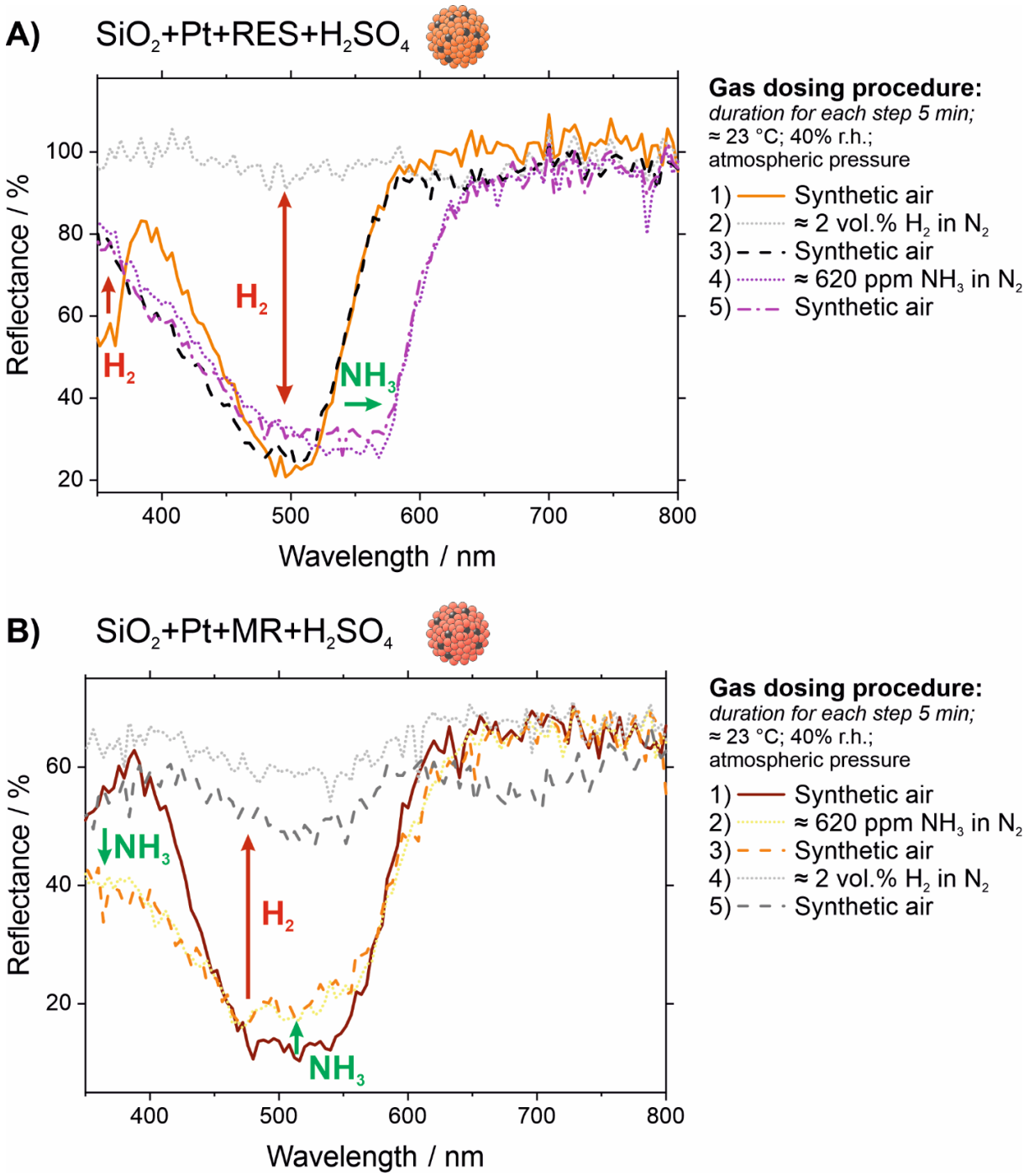

Fig. S13. (A-B) UV-vis reflectance spectra of H_2 indicator SPs consisting of SiO_2 NPs, Pt NPs, H_2SO_4, and the indicator dyes (A) RES and (B) MR, respectively during a defined gas dosing procedure, including H_2 dosing (≈ 2 vol.% H_2 in N_2) and NH_3 dosing (≈ 620 ppm NH_3 in N_2). H_2- and NH_3-induced spectral reflectance changes are indicated by coloured arrows.

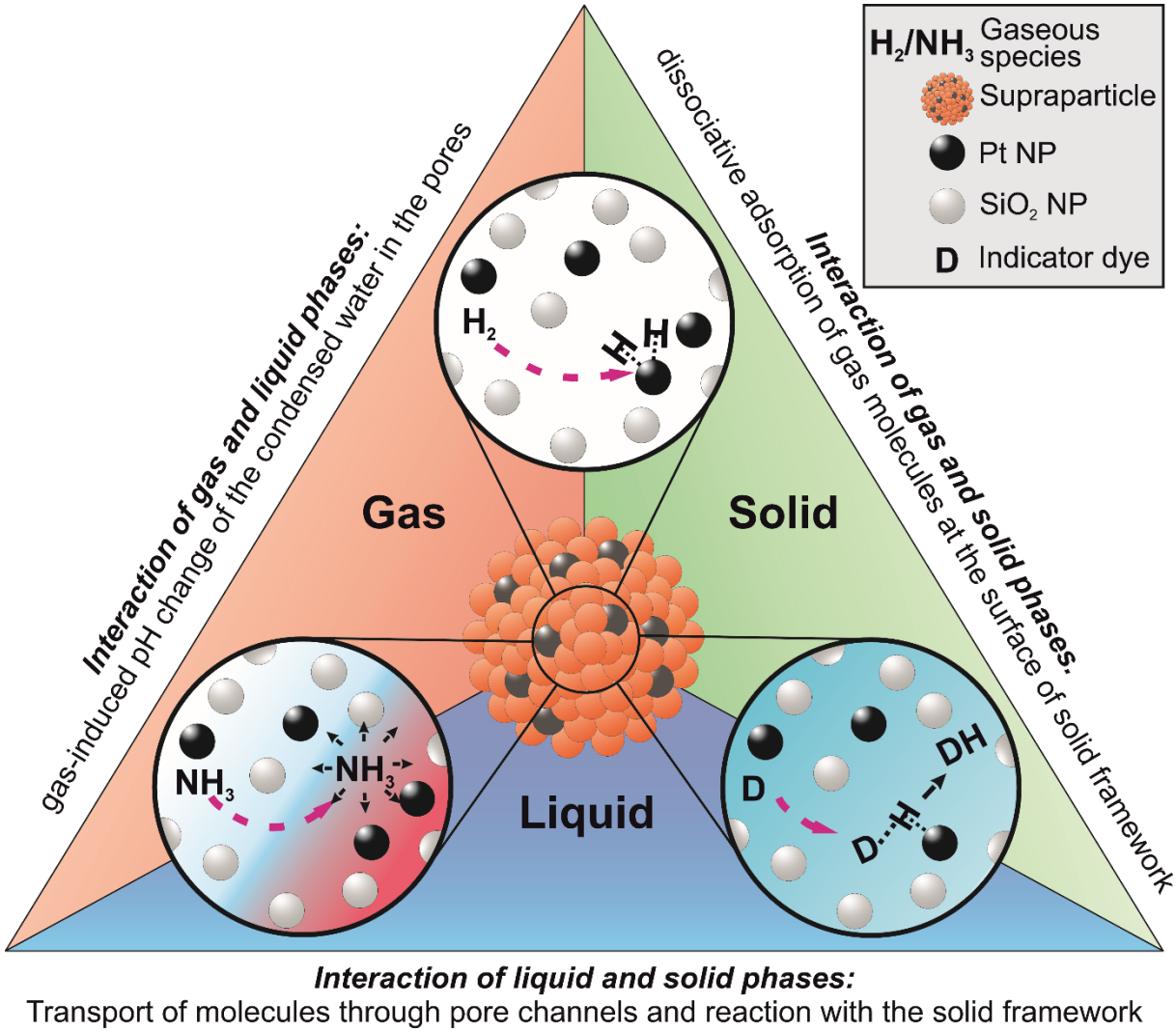

Fig. S14. Schematic illustration of the interaction potential within the solid-liquid-gas interface hosted by the mesopores of the conceptualized micron-sized SP, enabling the emergence of the targeted dual-gasochromic functionality for H_2 and NH_3 vapours.

Experimental section

Materials and reagents

Resazurin sodium salt (RES, $C_{12}H_6NNaO_4$, dye content ≈ 80%), sodium citrate dehydrate ($C_6H_5Na_3O_7 \cdot 2\ H_2O$, ≥ 99%), sodium borohydride ($NaBH_4$, 99%), tetrazolium red (TTZ, $C_{19}H_{15}ClN_4$, ≥ 98.0%), methylene blue (MB, $C_{16}H_{18}ClN_3S \cdot xH_2O$, dye content, ≥82%) and Reichardt's dye (RD, $C_{41}H_{29}NO$, 90%) were purchased from Sigma Aldrich. Dihydrogen hexachloroplatinate (IV) hydrate ($H_2PtCl_6 \cdot 6\ H_2O$, 99.9%) and bromocresol green (BG, $C_{21}H_{14}Br_4O_5S$, FTIR conforms was obtained from Alfa Aesar. Citric acid monohydrate ($C_6H_8O_7 \cdot H_2O$, > 99.5%),) and bromophenol blue (BPB, $C_{19}H_{10}Br_4O_5S$, ACS reagent) were received from ThermoFisher Scientific. Aqueous ammonia solution (NH_3+H_2O, 25%), sulphuric acid (H_2SO_4, 96%), methyl red (MR, $C_{15}H_{15}N_3O_2$, p.a., ACS) and bromothymol blue (BTB, $C_{27}H_{28}Br_2O_5S$, p.a., ACS) were purchased from Carl Roth. Phenolphthalein (PPT, $C_{20}H_{14}O_4$, ACS reagent) and thymolphthalein (TPT, $C_{28}H_{30}O_4$, ACS reagent) were obtained from Merck. Silica (SiO_2) NPs (Köstrosol 0830, KS0830) in the form of an aqueous, NaOH-stabilised NP dispersion (pH 10) containing 30 wt. % SiO_2 were received from Chemiewerke Bad Köstritz. All chemicals used without further purification. Water was deionized before usage. The purity of the purchased dye species was exemplarily investigated by ^{1}H-NMR spectroscopy. The recorded spectra of RES (Fig. S15) and MR (Fig. S16) using D_2O and DMSO-d6 as solvents confirm a purity of ≥ 98%.

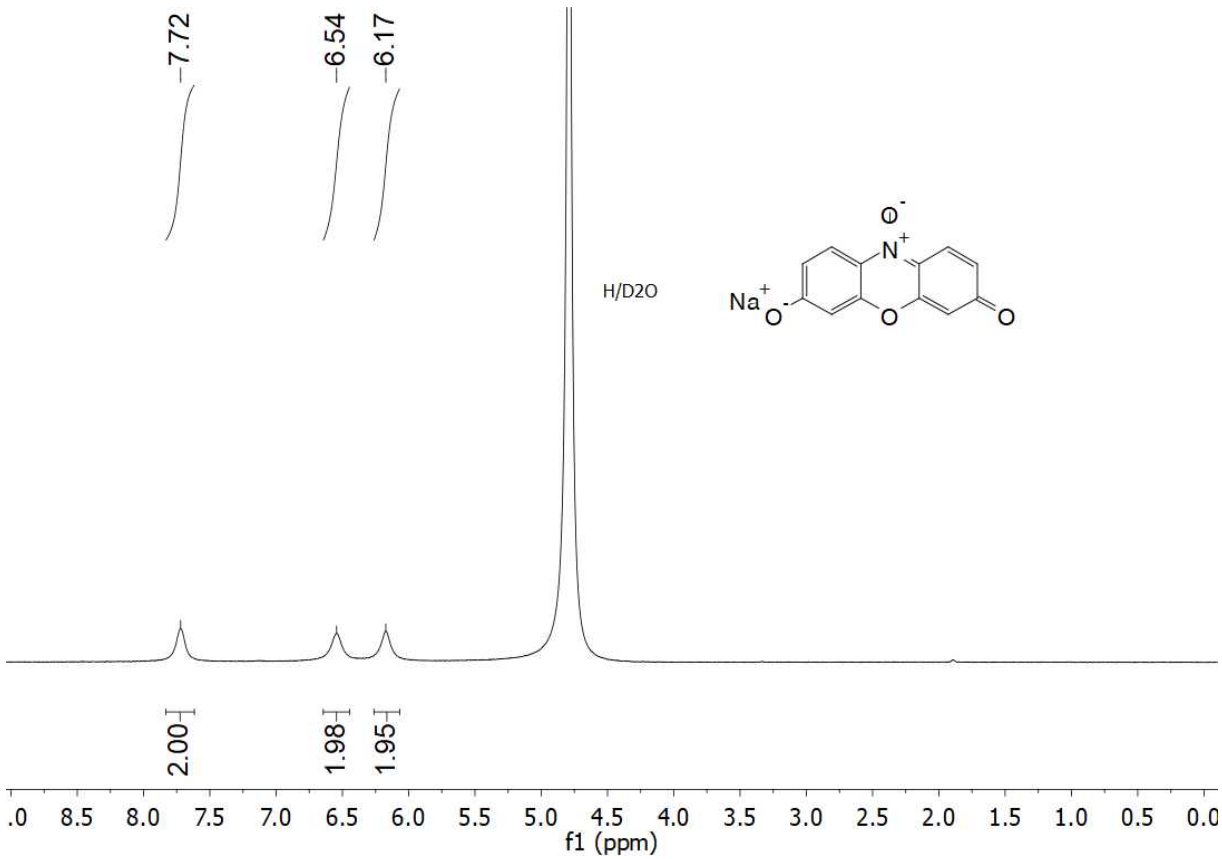

Fig. S15. ^{1}H-NMR spectrum of the resazurin (RES) dye used (Sigma-Aldrich) dissolved in D_2O.

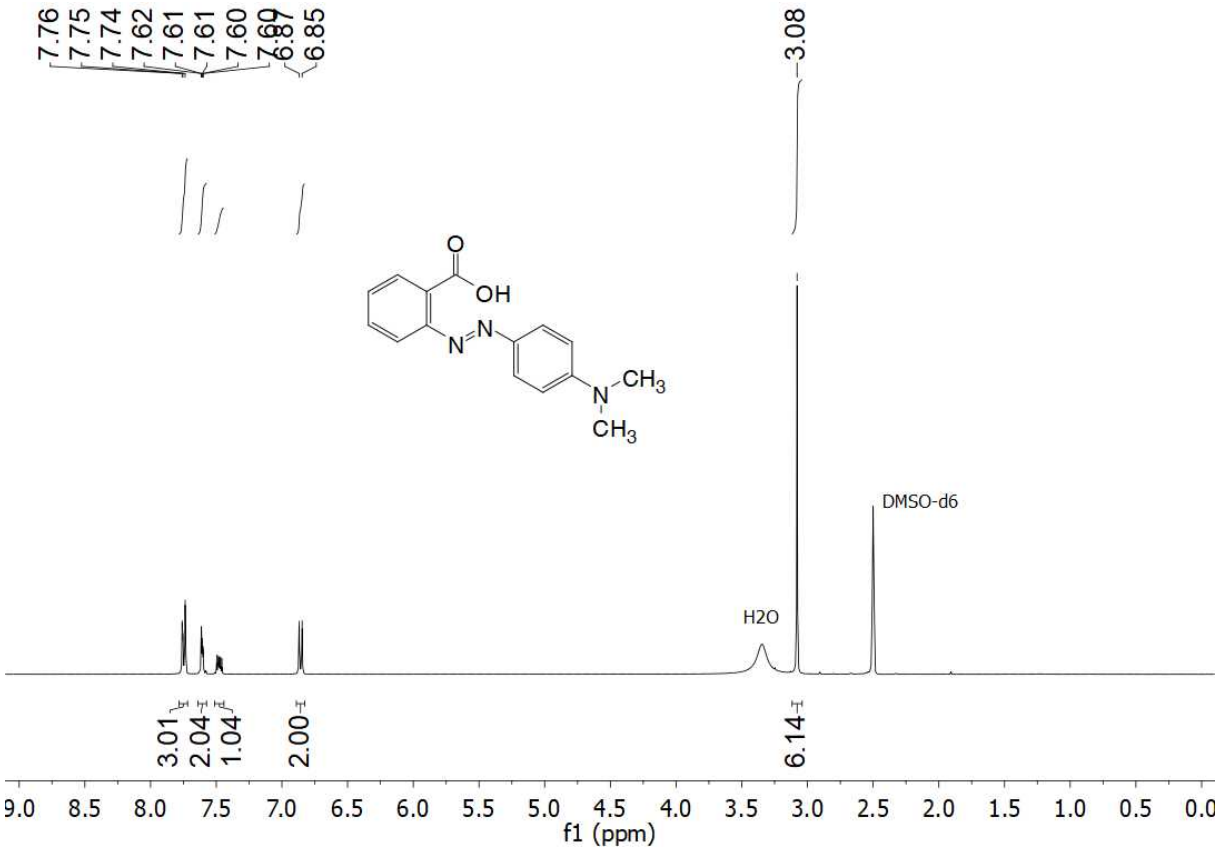

Fig. S16. ^{1}H-NMR spectrum of the methyl red (MR) dye used (Carl Roth) dissolved in DMSO-d6.

Synthesis of Pt NPs

Pt NPs were synthesized via a reduction of H_2PtCl_6 using $NaBH_4$ according to previous work from others[15] with slight adaptions made in our group[16]. A two neck round bottom flask was loaded with a solution of $H_2PtCl_6 \cdot 6\,H_2O$ (19.6 mg, 47 µmol) in H_2O (139 mL) and heated to 100 °C under reflux conditions. Subsequently, an aqueous solution containing 1 wt.% sodium citrate and 0.05 wt.% citric acid (1.1 mL) was added. The resulting mixture was stirred for 30 s. Afterwards, a freshly prepared mixture of $NaBH_4$ (13.0 mg; 0.34 mmol) and an aqueous solution containing 1 wt.% sodium citrate and 0.05 wt.% citric acid (0.55 mL) was added, resulting in a black dispersion. This dispersion was left to stir for another 2 min before cooling it down via an ice bath. The resulting dispersion was concentrated via rotary evaporation and purified via dialysis (cellulose membrane, ~10 to 20 kDa, Carl Roth) against 5 L of water (six water changes in 72 h).

Fabrication of SPs

First, a vial was loaded with a mixture containing SiO_2 NP dispersion (3.33 g, KS0830, 1 g NaOH-stabilized SiO_2 NPs, pH ≈ 10), an aqueous solution of the dye (RES, 5 mL, 1 mg·mL^{-1}; MR, 7.05 mL; 1 mg·mL^{-1} in H_2O:EtOH (1:1); – to achieve a constant molar dye concentration of 20 µmol·g^{-1} SP), Pt NPs (1 mL) and for the corresponding samples H_2SO_4 (2 mL; 2 wt.%). Subsequently, the mixture was sonicated in an ultrasonic bath (RK 514, Bandelin) for 10 min. Afterwards, the dispersion was spray-dried under continuous stirring using a lab-scale spray dryer (Büchi Labortechnik AG, B290 mini connected to a dehumidifier B-296). The parameters were kept constant for all samples and set to a pump rate of 10% (180 mL h^{-1}), an inlet temperature of 85 °C resulting in an outlet temperature of ≈48 °C, an aspirator power of 85% resulting in a volume flow of ≈33 m^3 h^{-1} (≈ 70 mbar pressure), and compressed air flow of≈ 480 L h^{-1}. The spray-drying processes yielded colourful powders depending on the used dyes and pH of the feed dispersion.

Material characterisation

^{1}H-NMR spectra of RES and MR were recorded on a Bruker Ascend 400 (^{1}H at 400 MHz) spectrometers using D_2O and DMSO-d6 as solvents.

The performed screening of the chromophore systems in the liquid phase is described in detail in the section "Chromophore systems" in the ESI. UV-vis spectra of aqueous dispersions containing dye molecules and Pt NPs were measured with a SPECORD 200 (AnalytikJena) in the wavelength range from 250-700 nm with a scan rate of 5 nm·s^{-1} and a data interval of 1 nm. Dynamic light scattering (DLS) measurements of diluted and freshly sonicated NP dispersions were carried out using a Zetasizer Nano (Malvern Panalytical) at 25 °C monitoring the scattering signal in a backscattering angle (173°).

SEM imaging analyses were performed on a JSM-F100 (JEOL) at a working distance of ≈5-6 mm using an acceleration voltage of 5 kV. The morphological analyses were carried out using a secondary electron detector. Elemental contrast imaging was facilitated via backscattered electron detection. For the morphological analyses, SP powders were placed on a carbon pad (Plano) and subsequently sputtered with Pt (108SE, Cressington). SP cross-sections were prepared by embedding SP powders between two silicon wafers and cutting with a cross-sectional polisher (IB-19530CP, JEOL) in a pulsed mode for 10 h. The Ar flow was set to 4.5 sccm and the ion accelerating voltage to 8 kV.

N_2 ad/desorption measurements at 77.4 K were carried out on a NOVAtouch LX2 sorption instrument (AntonPaar, Quantachrome instruments). The samples were dried at 120 °C and 4 mbar in a vacuum drying chamber (VO29, Memmert) for 16 h and outgassed at 140 °C for 12 h under vacuum before each measurement. H_2O adsorption experiments were performed at 298 K with a volumetric (manometric) sorption analyzer (Vstar, Anton Paar). Before each sorption measurement, the samples were outgassed for 12 h under a turbomolecular pump vacuum at 150 K and then weighed under an inert atmosphere. A second cycle (without any additional thermal treatment) was measured for the two SP samples to evaluate the non-closing hysteresis and hydroxylation of the surface during the first cycle.

To investigate and record the visual colour change of SPs, several mg of SP powder were placed in a glass vial (open system) and subjected to H_2 dosing from a 2 L gas bag (FisherScientific) that was connected to a 1 mL syringe and filled with H_2 (≥ 99.9%, AirLiquide). The H_2 dosing was performed at ambient conditions (air atmosphere, ≈23 °C, ≈30% r.h.) in one cycle of 20 s (flow rate: ≈10 mL·s^{-1}). NH_3 vapour dosing was performed by squeezing a spray bottle (500 mL) that was partially filled with 20-50 mL of an aqueous ammonia solution (30%) for 3 s. Importantly, the tube of the spray bottle was fixed in a position that

enabled vapour dosing without spilling any solution on the sample. The (ir)reversible colour change of the SP powders was recorded with a digital camera (Alpha6000, Sony), and snapshots of the videos were taken at characteristic times during the gas dosing procedure. It is important to note that due to the low relative humidity in the laboratory, some SP powders were additionally exposed to constant climate conditions (*ex situ* H_2O dosing, 1 h, 30 °C, 98% r.h.) in a climate chamber (MKF 56-E5, Binder) with activated dewing protection before recording the videos. The reversibility of the NH_3 detection was tested by dosing NH_3 vapours for 3 s and a subsequent recovery step of 2 to 3 min at ambient conditions in air atmosphere until another NH_3 dosing was performed. This process was repeated multiple times to reveal the indicator/sensor properties of the SP powder towards NH_3-induced deprotonation. Simultaneous dosing of both gases was performed by exposing the SP powders to H_2 for 10 s, which was followed by a concurrent dosing with NH_3 vapours for 10 s. Subsequently, the H_2 flow was continued for further 30 s. Consecutive dosing of H_2 and NH_3 vapours and vice versa was performed by first dosing one target species and after a 10 min recovery step at ambient conditions in air atmosphere, dosing the second species.

Fluorescence emission and excitation spectra were recorded with a FP-8500 spectrofluorometer (Jasco) using constant experimental parameters (excitation bandwidth: 5 nm; emission bandwidth: 5 nm, response time: 0.05 s, scan speed: 100 nm min^{-1}, data interval: 0.5 nm). Emission spectra were recorded using an excitation wavelength of 365 nm. Excitation spectra were recorded by monitoring the emission intensity of the respective sample at one specific wavelength and varying the excitation wavelength. A powder sample cell PH-002 was used for the measurements (quartz window size: 0.8 nm, Jasco). All recorded spectra were corrected using a calibrated WI light source ESC-842 (Jasco). All measurements were performed at almost constant climate conditions (≈ 23 °C, ≈30% relative humidity).

In situ UV-vis reflectance measurements of SP powders were performed with a UV/VIS/NIR spectrometer (Lamda 900, Perkin Elmer) using a reflection setup (Praying Mantis, Harrick Scientific) for probes with diffuse surfaces and a tungsten lamp. Home-built powder sample holders and roughly 10 mg of SPs were used for the sample preparation. UV-vis spectra were recorded in the wavelength range from 800-350 nm. The screening was performed with a data interval of 4 nm, a scan rate of 387 nm·min^{-1}, and an integration time of 0.52 s at atmospheric pressure and RT (≈ 23 °C). The gas dosing was performed with a home-built setup connected to different gas bottles (100% N_2, 100% O_2, 3.46% H_2 in N_2 and 1040 ppm NH_3 in N_2; all purchased from Linde GmbH) with individual mass flow controllers (flow rates: 10-200 ml·min^{-1}). The total gas flow was kept constant at 200 mL·min^{-1} throughout all experiments. The relative humidity of the gas flow was controlled by dosing N_2 saturated with H_2O via a bubbler system (the H_2O reservoir was kept at room temperature, RT). The detailed gas dosing procedures were depicted in Fig. S10. Air dosing was performed with 80 mL·min^{-1} N_2, 80 mL·min^{-1} H_2O-satturated N_2 and 40 mL·min^{-1} O_2. H_2 dosing was carried out with 120 mL·min^{-1} 3.46% H_2 in N_2 and 80 mL·min^{-1} H_2O-satturated N_2. NH_3 dosing was conducted with 120 mL·min^{-1} 1040 ppm NH_3 in N_2 and 80 mL·min^{-1} H_2O-satturated N_2.

Author Contributions

A.Z. and J.R. contributed equally.

A.Z., J.R. (Conceptualization: Lead; Investigation: Lead, Methodology: Lead; Supervision: Lead; Validation: Lead; Visualization: Lead; Writing – original draft: Lead; Writing – review & editing: Lead). N.R., N.S., C.C.C. (Investigation: Equal, Writing – review & editing: Equal), B.S.M., M.T., E.A.K., S.W. (Writing – review & editing: Equal), K.M. (Conceptualization: Lead; Funding acquisition: Equal; Project administration: Lead; Resources: Lead; Supervision: Equal; Writing – review & editing: Equal). All authors have approved the final version of the manuscript.

References

1 M. E. Smith, A. L. Stastny, J. A. Lynch, Z. Yu, P. Zhang and W. R. Heineman, *Anal. Chem.*, 2020, **92**, 10651.
2 S. Khazalpour and D. Nematollahi, *RSC Adv.*, 2014, **4**, 8431.
3 M. Thommes, K. Kaneko, A. V. Neimark, J. P. Olivier, F. Rodriguez-Reinoso, J. Rouquerol and K. S.W. Sing, *Pure Appl. Chem.*, 2015, **87**, 1051.
4 J. Reichstein, S. Schötz, M. Macht, S. Maisel, N. Stockinger, C. C. Collados, K. Schubert, D. Blaumeiser, S. Wintzheimer, A. Görling, M. Thommes, D. Zahn, J. Libuda, T. Bauer and K. Mandel, *Adv. Funct. Mater.*, 2022, **32**, 2112379.
5 K. Zhang, J. Reichstein, P. Groppe, S. Schoetz, N. Stockinger, J. Libuda, K. Mandel, S. Wintzheimer and T. Retzer, *Chem. Mater.*, 2023, **35**, 6808.
6 G. Marzun, C. Streich, S. Jendrzej, S. Barcikowski and P. Wagener, *Langmuir*, 2014, **30**, 11928.
7 K. B. Kiradjiev, V. Nikolakis, I. M. Griffiths, U. Beuscher, V. Venkateshwaran and C. J. W. Breward, *Ind. Eng. Chem. Res.*, 2020, **59**, 4802.
8 D. Ibáñez, D. Izquierdo-Bote, A. Pérez-Junquera, M. B. González-García, D. Hernández-Santos and P. Fanjul-Bolado, *Dyes Pigments*, 2020, **172**, 107848.
9 Y. Zhou, W. Wei, H. Su and W. Wang, *Inorg. Chem. Commun.*, 2019, **106**, 139.
10 C. Bueno, M. L. Villegas, S. G. Bertolotti, C. M. Previtali, M. G. Neumann and M. V. Encinas, *Photochem. Photobiol.*, 2002, **76**, 385.
11 D. A. Finkelstein, E. Bertin, S. Garbarino and D. Guay, *J. Phys. Chem. C*, 2015, **119**, 9860.
12 G. Xu, J. J. O'Dea and J. G. Osteryoung, *Dyes Pigments*, 1996, **30**, 201.
13 T. Hübert, L. Boon-Brett, G. Black and U. Banach, *Sens. Actuators B Chem.*, 2011, **157**, 329.
14 Rana Prathap Padappayil and Judith Borger, in *StatPearls [Internet]*, ed. R. P. Padappayil and J. Borger, StatPearls Publishing, 2023.
15 N. C. Bigall, T. Härtling, M. Klose, P. Simon, L. M. Eng and A. Eychmüller, *Nano Lett.*, 2008, **8**, 4588.
16 a) K. Zhang, J. Reichstein, P. Groppe, S. Schötz, N. Stockinger, J. Libuda, K. Mandel, S. Wintzheimer and T. Retzer, *Chem. Mater.*, 2023, **35**, 6808; b) K. Zhang, S. Schötz, J. Reichstein, P. Groppe, N. Stockinger, S. Wintzheimer, K. Mandel, J. Libuda and T. Retzer, *J. Chem. Phys.*, 2023, **158**, 134722;